

# Friction and Shear Strength at the Nanowire-Substrate Interfaces

Yong Zhu<sup>1\*</sup>, Qingquan Qin<sup>1</sup>, Yi Gu<sup>2</sup> and Zhong Lin Wang<sup>3</sup>

<sup>1</sup> Department of Mechanical and Aerospace Engineering, North Carolina State University, Raleigh, North Carolina 26795

<sup>2</sup> Department of Physics, Washington State University, Pullman, Washington 99164

<sup>3</sup> School of Materials Science and Engineering, Georgia Institute of Technology, Atlanta, Georgia 30332

## Abstract

The friction and shear strength of nanowire (NW)–substrate interfaces critically influences the electrical/mechanical performance and life time of NW-based nanodevices. Yet, very few reports on this subject are available in the literature because of the experimental challenges involved and no studies have been reported to investigate the configuration of individual NW tip in contact with a substrate. In this letter, using a new experimental method, we report the friction measurement between a NW tip and a substrate for the first time. The measurement was based on NW buckling *in-situ* inside a scanning electron microscope. The coefficients of friction between silver NW and gold substrate and between ZnO NW and gold substrate were found to be 0.09-0.12 and 0.10-0.15, respectively. The adhesion between a NW and the substrate modified the true contact area, which affected the interfacial shear strength. Continuum mechanics calculation found that interfacial shear strengths between silver NW and gold substrate and between ZnO NW and gold substrate were 134-139 MPa and 78.9-95.3 MPa, respectively. This method can be applied to measure friction parameters of other NW-substrate systems. Our results on interfacial friction and shear strength have direct implication on the AFM three-point bending tests used for nanomechanical characterization.

**Keywords:** nanowire, interface, friction, shear strength, nanomechanics

\* Author to whom correspondence should be addressed; electronic mail:

yong\_zhu@ncsu.edu

## 1. Introduction

In nanodevices, nanowires (NWs) are typically integrated to larger structures. The NW-substrate interfaces therefore play a critical role in both mechanical reliability and electrical performance of these nanodevices, especially when the size of the NW is small<sup>1,2</sup>. Such interfaces include two configurations, NW length or NW tip in contact with the substrate, and both configurations have a wide range of applications. For example, the tip-substrate contacts are present in nanogenerators<sup>3</sup>, nanostructured solar cells<sup>4</sup>, Atomic force microscopy (AFM) with carbon nanotube (CNT) tips<sup>5</sup>, CNT tapes<sup>6</sup> and many other nanodevices. Indeed, as recently outlined by Wang<sup>7</sup>, one critical future direction for nanogenerator research is study of the NW-metal interface to build a robust, low wearing structure for improving the device lifetime.

Experimental work on NW interfacial mechanics has been limited so far due to experimental challenges at the nanoscale<sup>8</sup> and the fact that many existing tribology tools such as AFM, surface force apparatus (SFA), quartz microbalance and microfabricated devices cannot be readily applied<sup>9, 10</sup>. Static friction force between NWs (including CNTs) and substrates was estimated from the highly deformed shapes of NWs<sup>11</sup>. Recently CNTs were found to slip on silicon oxide surface at a lateral force of 8 nN<sup>12</sup>, and ZnO NWs to slip on silicon surface at a few  $\mu\text{N}$ <sup>13</sup>. However, the above studies on friction are only limited to the configuration of NW length in contact with a substrate. To the best of our knowledge, no experiments have been reported to investigate the configuration of individual NW tip in contact with a substrate.

Here we report the first experimental study on the friction between NW tips (ends) and a substrate. Silver and ZnO NWs with a gold-coated substrate were studied as model systems in view that silver and ZnO NWs have very different tip shapes. Silver NW is an important class of metallic NWs because of its potential use as interconnects in view that bulk silver exhibits the

highest electrical and thermal conductivity among all metals<sup>14</sup>. ZnO is one of the most important semiconductor NWs with a broad range of applications including nanogenerators, biosensors, nanolasers and nanoelectromechanical systems (NEMS)<sup>15</sup>. The friction measurements reported in this paper were enabled by an innovative experimental method based on column buckling theory. The experiments were conducted *in-situ* inside a scanning electron microscope (SEM) using a nanomanipulator as the actuator and an AFM cantilever as the force sensor.

## 2. Experimental

The silver NWs were synthesized using a seed-assisted, solution-phase method with a five-fold twin structure<sup>16</sup>. Figure 1(a) is a transmission electron microscopy (TEM) image showing the NW tip. Figure 1(b) and 1(c) are high-resolution TEM images showing a layer of silver oxide with varying thickness on the NW surface. The ZnO NWs were synthesized using the vapor-liquid-solid (VLS) method with a wurtzite structure and growth direction of [0001]<sup>17</sup>. Figure 1(d) is a SEM image showing the tip of a ZnO NW, which appears to be flat.

*In situ* SEM buckling tests of NWs were conducted as shown in Figure 2. A nanomanipulator (Klocke Nanotechnik, Germany) that possesses 1 nm resolution in three orthogonal directions was used to pick up individual NWs<sup>18, 19</sup>. A NW was clamped onto the tungsten tip on the nanomanipulator using electron beam induced deposition (EBID) of carbon. Then the NW was approached to make contact with an AFM cantilever (OBL-10, Veeco). Carbon deposition was not employed at the NW-cantilever interface. Compressive force was applied to the NW by the nanomanipulator movement, which led to buckling of the NW. In this case, the boundary condition was fixed-pinned. Continued loading further changed the postbuckling shape of the NW until sliding occurred at the NW-cantilever interface.

After buckling of the NW, there exist two forces at the NW-substrate interface, a compressive (normal) force and a frictional (lateral) force. The compressive force on the NW can be easily measured from the deflection of the AFM cantilever; however it is not trivial to measure the friction force. Below we describe a method to measure friction force based on the buckling theory. Free-body diagram of a buckled member under fixed-pinned boundary condition is shown in Figure 3(a), with the left end fixed and the right end pinned. A small lateral deflection gives rise to a moment  $M$  at the fixed end and shear force (friction force)  $F$  at each end of the member. From the moment balance, it can be easily obtained that  $F = M / L$ , where  $L$  is the length of the member. The governing equation at a section with a distance  $x$  from the right end is given by

$$y''+k^2 y = \frac{M}{EI} \frac{x}{L} \quad (1)$$

where  $k^2 = P / EI$ ,  $E$  is the Young's modulus and  $I$  is the moment of inertia. The solution to Eq. (1) is

$$y = A \sin kx + B \cos kx + \frac{M}{P} \frac{x}{L} \quad (2)$$

Taking into account the fixed-pinned boundary condition, we obtain

$$y = \frac{M}{P} \left[ \frac{x}{L} + 1.02 \sin(4.49 \frac{x}{L}) \right] \quad (3)$$

Eq. (3) describes the shape of the member in the postbuckling stage. Details on the equation derivation can be found elsewhere<sup>20</sup>. Eq. (3) provides the theoretical basis of our method to measure the friction force. By fitting the observed shape of the NW just prior to sliding to Eq. (3) using the nonlinear least squares method,  $M$  can be determined since  $P$  is measured from the deflection of the AFM cantilever. Then  $F$  can be obtained using  $F = M / L$ . Figure 3(b) shows the fitting of a deformed NW to Eq. (3). Clearly the agreement is very good.

### 3. Results and Discussion

Following the method describe above, three silver NWs and three ZnO NWs were tested for friction measurements. The Amonton–Coulomb friction law is written as  $F = \mu P$ , where  $\mu$  is the so-called coefficient of friction. The normal force, friction force and coefficient of friction for all six NWs are listed in Table 1. Note that these NWs did not break in the buckling experiments so that each NW was tested multiple times with very good repeatability. However, the Amonton–Coulomb law was obtained from empirical observations with many counterexamples; for instance, geckos are able to move on walls and ceilings when  $P \leq 0$ . A more fundamental friction law that links friction and adhesion was proposed by Bowden and Tabor<sup>21</sup>,

$$F = \tau A \quad (4)$$

where  $\tau$  is the interfacial shear strength and  $A$  is the true contact area. This law has been supported by numerous SFA and AFM experiments<sup>10</sup>. The two theories were reconciled by considering the multiple asperities among the contacting surfaces<sup>22</sup>; as a result the true contact area is typically proportional to the normal force.

The NW-substrate contact is treated as the single-asperity contact because the NW diameters are smaller than the wavelength of the substrate topography. In order to evaluate interfacial shear strength using Eq. (4), the true contact area must be determined. In our experiments as well as AFM experiments, the true contact area is calculated using continuum mechanics models. The well-known Hertzian model does not take into account attractive adhesion forces between the contacting surfaces. Other widely-accepted models that take adhesion force into account are due to Johnson, Kendall, and Roberts (JKR)<sup>23</sup>, Derjaguin, Muter, Toporov (DMT)<sup>24</sup> and Maugis<sup>25</sup>, respectively.

For simplicity, the continuum models typically assume the contact between a sphere and a flat surface. It is known that the JKR and DMT theories are two extremes of a spectrum of elastic solutions determined by the Tabor parameter<sup>26</sup>, which is given by

$$\mu = \left( \frac{16R\gamma^2}{9K^2z_0^3} \right)^{1/3} \quad (5)$$

where  $R$  is the radius of the sphere,  $K$  is the reduced modulus of two materials  $K = 4/3[(1-\nu_1^2)/E_1 + (1-\nu_2^2)/E_2]^{-1}$  with  $E_1$  and  $E_2$  the respective Young's moduli, and  $\nu_1$  and  $\nu_2$  the respective Poisson's ratios,  $z_0$  is the interatomic equilibrium distance ( $= 0.2$  nm),  $\gamma$  is the interfacial energy per unit area (work of adhesion). Each NW tip was fitted with a sphere. When  $\mu > 5$ , the JKR model is valid; when  $\mu < 0.1$ , the DMT model should be applied; in the intermediate range, the Maugis model becomes appropriate. In all our experiments  $2.05 < \mu < 2.39$  (see Table 2), so the Maugis model should be used. However, the Maugis model does not have an explicit expression for contact radius. For the Tabor parameter in this range, the JKR model was found to approximate the Maugis solution very closely<sup>27</sup>, therefore the JKR model was used in our calculation due to its simplicity.

Following the Hertz and JKR models, the contact radius  $a$  as a function of the externally applied load  $P$  is given by

$$a = \left[ \frac{PR}{K} \right]^{1/3} \quad (6a)$$

$$a = \left[ \frac{R}{K} \left( P + 3\gamma\pi R + \sqrt{6\gamma\pi RP + (3\gamma\pi R)^2} \right) \right]^{1/3} \quad (6b)$$

respectively, where  $\gamma = \gamma_1 + \gamma_2 - \gamma_{12} \approx 2\sqrt{\gamma_1\gamma_2}$  with  $\gamma_1$  and  $\gamma_2$  the respective surface energy and  $\gamma_{12}$  the interface energy.  $\gamma_1 = 1.37 J/m^2$  for gold,  $\gamma_2 = 0.8 J/m^2$  for silver oxide<sup>28</sup> and

$\gamma_2 = 1.74 J/m^2$  for ZnO with {0001} surface<sup>29</sup>. Therefore,  $\gamma = 2.09 J/m^2$  and  $\gamma = 3.09 J/m^2$  for the contacts between gold and silver oxide and between gold and ZnO, respectively. In addition,  $E_{gold} = 78 GPa$ ,  $E_{silver} = 84 GPa$ ,  $E_{ZnO} = 140 GPa$ ,  $\nu_{gold} = 0.44$ ,  $\nu_{silver} = 0.37$ ,  $\nu_{ZnO} = 0.30$ <sup>30</sup>. The contact radius, contact pressure and interfacial shear strength calculated using the two models are listed in Table 2. It can be seen that the interfacial shear strengths between silver NW and gold substrate and between ZnO NW and gold substrate are 134-139 MPa and 78.9-95.3 MPa, respectively. These values are in good agreement with those obtained from AFM and mesoscale friction tester in similar environment (vacuum or dry)<sup>31</sup>.

Several issues related to the experiments and analyses are discussed. First of all, our measurements showed that no metallic bonding formed between silver NWs and the gold substrate as the strength of metallic bonding is typically on the order of GPa<sup>32</sup>. This is due to the presence of a thin layer of silver oxide, as shown in the high-resolution TEM images (Figure 1). Second, it is not appropriate to treat the ZnO NWs as the molecular junctions where the contact areas remain constant (in our case the NW cross sections)<sup>33</sup>, otherwise the interfacial shear strength would be too small. This is reasonable because it is very likely that the NW is not perfectly perpendicular to the substrate. Edge of the NW tip is in contact with the substrate, and the contact area can then be approximately fitted with a sphere. Third, previous experiments showed that electron beam increases adhesion force between semiconductors and metals<sup>34, 35</sup>. For contacts between ZnO NW tips and a gold substrate, we found the adhesion force did not show noticeable change when the contact area was exposed to electron beam only for a short time (e.g., less than 10 seconds)<sup>36</sup>. Last, although our experimental method gave rise to the first measurement of the friction data between NW tips and a substrate, we are aware that it cannot

measure the friction as a function of the progressively-applied normal force. MEMS devices with normal and lateral force measurement capability are under development to address this issue.

Our results on interfacial friction and shear strength have direct implication on the AFM three-point bending tests that are widely used in extracting mechanical properties of one-dimensional nanostructures including CNTs and NWs<sup>37, 38</sup>. Often the adhesion between the NWs and the substrate is assumed to be strong enough to provide a fixed-fixed boundary condition for the three-point bending tests. The assumption is valid for NWs with small diameters; but for those with large diameters, it could lead to large data scatter typically observed in experiments. Our results could be incorporated into data reduction in the three-point bending experiments to quantify the influence of adhesion and friction on the measured mechanical properties. Other methods could also be used to eliminate the ambiguity caused by the NW-substrate friction such as EBID of platinum or carbon in SEM<sup>39</sup>.

#### **4. Conclusions**

In summary, a new experimental method to measure the friction between a NW tip and a substrate has been developed. Silver and ZnO NWs were tested with a gold coated surface as the substrate. The coefficients of friction between silver NW and gold substrate and between ZnO NW and gold substrate were found to range from 0.09 to 0.12 and from 0.10 to 0.15, respectively. The adhesion between NWs and the substrate substantially modified the true contact area, which in turn affected the interfacial shear strength significantly. According to the calculated Tabor parameter, the JKR model was selected to approximately calculate the contact area and the interfacial shear strength. The interfacial shear strengths between silver NW and gold substrate and between ZnO NW and gold substrate ranged from 134 to 139 MPa and from

78.9 to 95.3 MPa, respectively. These values are in good agreement with previous results obtained in similar environment (vacuum or dry)<sup>31</sup>.

## Acknowledgement

This work was supported by the National Science Foundation under Award No. CMMI-0826341 and the Faculty Research and Professional Development Fund from North Carolina State University. Thanks to Fengru Fan and Afsoon Souidi for kindly providing the NW samples.

## Reference

1. Lu, W.; Lieber, C. M., Semiconductor nanowires. *Journal of Physics D-Applied Physics* **2006**, 39, (21), R387-R406.
2. Patolsky, F.; Lieber, C. M., Nanowires nanosensors. *Materials today* **2005**, 20-28.
3. Wang, Z. L.; Song, J. H., Piezoelectric nanogenerators based on zinc oxide nanowire arrays. *Science* **2006**, 312, (5771), 242-246.
4. Law, M.; Greene, L. E.; Johnson, J. C.; Saykally, R.; Yang, P. D., Nanowire dye-sensitized solar cells. *Nature Materials* **2005**, 4, (6), 455-459.
5. Dai, H. J.; Hafner, J. H.; Rinzler, A. G.; Colbert, D. T.; Smalley, R. E., Nanotubes as nanoprobe in scanning probe microscopy. *Nature* **1996**, 384, (6605), 147-150.
6. Ge, L.; Sethi, S.; Ci, L.; Ajayan, P. M.; Dhinojwala, A., Carbon nanotube-based synthetic gecko tapes. *Proceedings of the National Academy of Sciences of the United States of America* **2007**, 104, (26), 10792-10795.
7. Wang, Z. L., Towards Self-Powered Nanosystems: From Nanogenerators to Nanopiezotronics. *Advanced Functional Materials* **2008**, 18, (22), 3553-3567.
8. Falvo, M. R.; Superfine, R., Mechanics and Friction at the Nanometer Scale *Journal of Nanoparticle Research* **2000**, 2, 237-248.
9. Corwin, A. D.; de Boer, M. P., Effect of adhesion on dynamic and static friction in surface micromachining. *Applied Physics Letters* **2004**, 84, (13), 2451-2453.
10. Carpick, R. W.; Salmeron, M., Scratching the surface: Fundamental investigations of tribology with atomic force microscopy. *Chemical Reviews* **1997**, 97, (4), 1163-1194.
11. Conache, G.; Gray, S. M.; Ribayrol, A.; Froberg, L. E.; Samuelson, L.; Pettersson, H.; Montelius, L., Friction Measurements of InAs Nanowires on Silicon Nitride by AFM Manipulation. *Small* **2009**, 5, (2), 203-207.
12. Whittaker, J. D.; Minot, E. D.; Tanenbaum, D. M.; McEuen, P. L.; Davis, R. C., Measurement of the adhesion force between carbon nanotubes and a silicon dioxide substrate. *Nano Letters* **2006**, 6, (5), 953-957.
13. Manoharan, M. P.; Haque, M. A., Role of adhesion in shear strength of nanowire-substrate interfaces. *Journal of Physics D-Applied Physics* **2009**, 42, (9).

14. Sun, Y. G.; Mayers, B.; Herricks, T.; Xia, Y. N., Polyol synthesis of uniform silver nanowires: A plausible growth mechanism and the supporting evidence. *Nano Letters* **2003**, 3, (7), 955-960.
15. Wang, Z. L., Zinc oxide nanostructures: growth, properties and applications. *Journal of Physics-Condensed Matter* **2004**, 16, (25), R829-R858.
16. Fan, F. R.; Ding, Y.; Liu, D. Y.; Tian, Z. Q.; Wang, Z. L., Facet-Selective Epitaxial Growth of Heterogeneous Nanostructures of Semiconductor and Metal: ZnO Nanorods on Ag Nanocrystals. *Journal of American Chemical Society* **2009**, DOI: 10.1021/ja9036324.
17. Xu, F.; Qin, Q. Q.; Gu, Y.; Zhu, Y., Size Effects on Mechanical Properties of ZnO Nanowires under Tension and Buckling. **2009**, submitted.
18. Zhu, Y.; Espinosa, H. D., An electromechanical material testing system for in situ electron microscopy and applications. *Proceedings of the National Academy of Sciences of the United States of America* **2005**, 102, (41), 14503-14508.
19. Zhu, Y.; Xu, F.; Qin, Q. Q.; Fung, W. Y.; Lu, W., Mechanical Properties of Vapor-Liquid-Solid Synthesized Silicon Nanowires. *Nano Letters* **2009**, ASAP, DOI: 10.1021/nl902132w.
20. Chajes, A., *Principles of Structural Stability Theory*. Prentice-Hall: Englewood Cliffs, NJ, 1974.
21. Bowden, F. P.; Tabor, D., *The friction and lubrication of solids*. Oxford University Press: Oxford, UK, 1954.
22. Greenwood, J. A.; Williams, J. B. P., Contact of Nominally Flat Surfaces. *Proceedings of the Royal Society of London Series a-Mathematical and Physical Sciences* **1966**, 295, (1442), 300-&.
23. Johnson, K. L.; Kendall, K.; Roberts, A. D., Surface Energy and Contact of Elastic Solids. *Proceedings of the Royal Society of London Series a-Mathematical and Physical Sciences* **1971**, 324, (1558), 301-&.
24. Derjaguin, B. V.; Muller, V. M.; Toporov, Y. P., Effect of Contact Deformations on Adhesion of Particles. *Journal of Colloid and Interface Science* **1975**, 53, (2), 314-326.
25. Maugis, D., Adhesion of Spheres - the Jkr-Dmt Transition Using a Dugdale Model. *Journal of Colloid and Interface Science* **1992**, 150, (1), 243-269.
26. Tabor, D., Surface Forces and Surface Interactions. *Journal of Colloid and Interface Science* **1977**, 58, (1), 2-13.
27. Carpick, R. W.; Ogletree, D. F.; Salmeron, M., A general equation for fitting contact area and friction vs load measurements. *Journal of Colloid and Interface Science* **1999**, 211, (2), 395-400.
28. Israelachvili, J. N., *Intermolecular and Surface Forces*. 2nd ed.; Academic Press: Amsterdam, 1991.
29. Kim, M.; Hong, Y. J.; Yoo, J.; Yi, G. C.; Park, G. S.; Kong, K. J.; Chang, H., Surface morphology and growth mechanism of catalyst-free ZnO and Mg<sub>x</sub>Zn<sub>1-x</sub>O nanorods. *Physica Status Solidi-Rapid Research Letters* **2008**, 2, (5), 197-199.
30. Lucas, M.; Mai, W.; Yang, R.; Wang, Z. L.; Riedo, E., Aspect ratio dependence of the elastic properties of ZnO nanobelts. *Nano Letters* **2007**, 7, (5), 1314-1317.
31. Xu, D. W.; Ravi-Chandar, K.; Liechti, K. A., On scale dependence in friction: Transition from intimate to monolayer-lubricated contact. *Journal of Colloid and Interface Science* **2008**, 318, (2), 507-519.

32. Bhushan, B., *Nanotribology and Nanomechanics: An Introduction*. Springer: Heidelberg, 2008.
33. Li, Q. Y.; Kim, K. S., Micromechanics of friction: effects of nanometre-scale roughness. *Proceedings of the Royal Society a-Mathematical Physical and Engineering Sciences* **2008**, 464, (2093), 1319-1343.
34. Miyazaki, H. T.; Tomizawa, Y.; Saito, S.; Sato, T.; Shinya, N., Adhesion of micrometer-sized polymer particles under a scanning electron microscope. *Journal of Applied Physics* **2000**, 88, (6), 3330-3340.
35. Ding, W. Q., Micro/nano-particle manipulation and adhesion studies. *Journal of Adhesion Science and Technology* **2008**, 22, (5-6), 457-480.
36. Qin, Q. Q.; Xu, F.; Zhu, Y., Adhesion between zinc oxide nanowires and gold coated surfaces. **2009**, submitted.
37. Salvétat, J. P.; Briggs, G. A. D.; Bonard, J. M.; Bacsá, R. R.; Kulik, A. J.; Stockli, T.; Burnham, N. A.; Forro, L., Elastic and shear moduli of single-walled carbon nanotube ropes. *Physical Review Letters* **1999**, 82, (5), 944-947.
38. Ni, H.; Li, X. D.; Gao, H. S., Elastic modulus of amorphous SiO<sub>2</sub> nanowires. *Applied Physics Letters* **2006**, 88, (4).
39. Zhu, Y.; Ke, C.; Espinosa, H. D., Experimental techniques for the mechanical characterization of one-dimensional nanostructures. *Experimental Mechanics* **2007**, 47, (1), 7-24.

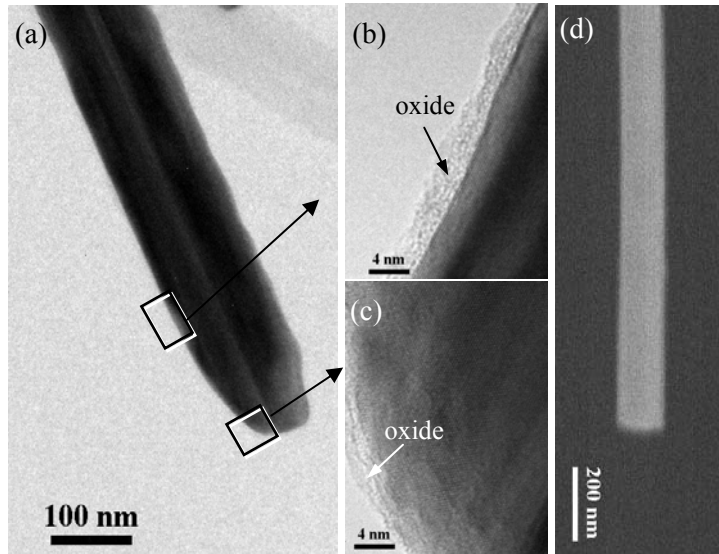


Figure 1. (a-c) TEM images of a silver NW. (b) and (c) show an oxide layer on the surface of the silver NW. (d) SEM image of a ZnO NW.

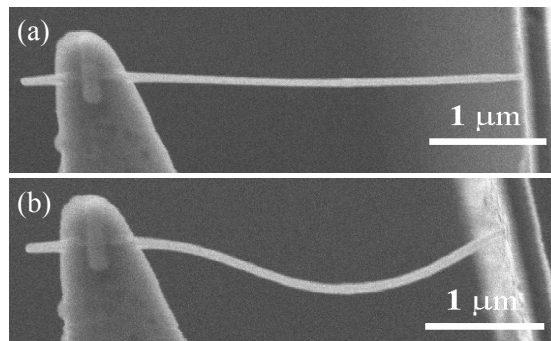


Figure 2. Buckling process of an individual NW. (a) is before buckling and (b) is after buckling and just prior to sliding on the right end.

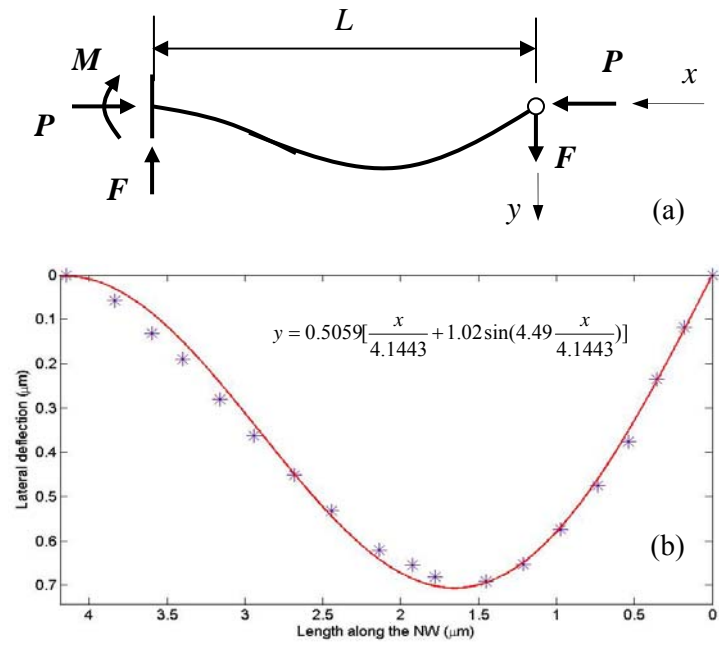


Figure 3. (a) Free-body diagram of a buckled column with fixed-pinned boundary condition. (b) Nonlinear least squares fitting of Eq. (3) to digitized shape of a NW prior to sliding.

Table 1. Normal force, friction force and coefficient of friction in each experiment.

Sample	Silver 1	Silver 2	Silver 3	ZnO 1	ZnO 2	ZnO 3
Normal force $P$ (nN)	263	277	465	186	203	215
Friction force $F$ (nN)	32.5	31.7	40.0	18.6	30.8	21.1
Coefficient of friction $\mu$	0.12	0.11	0.09	0.10	0.15	0.10

Table 2. Contact pressure and interfacial shear strength using the Hertz and JKR models.

Sample	Silver 1	Silver 2	Silver 3	ZnO 1	ZnO 2	ZnO 3
Tip radius $R$ (nm)	27	27	29	25	40	25
Tabor's parameter	2.28	2.28	2.33	2.05	2.39	2.05

Hertz model

Contact radius $a$ (nm)	4.79	4.87	5.93	3.90	4.69	4.09
Contact pressure (GPa)	3.65	3.72	4.21	3.90	2.94	4.09
Shear stress $\tau$ (MPa)	451	425	362	390	445	402

JKR model

Contact radius $a$ (nm)	8.64	8.68	9.58	8.32	11.1	8.40
Contact pressure (GPa)	1.21	1.17	1.61	0.86	0.52	0.97
Shear stress $\tau$ (MPa)	139	134	139	85.6	78.9	95.3